Hindawi
International Journal of Polymer Science
Volume 2019, Article ID 7379368, 7 pages
https://doi.org/10.1155/2019/7379368

Research Article

Synthesis of an Acrylamide Copolymer Containing Nano-SiO_2 by Ex Situ Cu(0)-Mediated SET-LRP

Ling Wang, Zhendong Li, Pingsen Huang, and Wei Ding

Provincial Key Laboratory of Oil & Gas Chemical Technology, Chemistry and Chemical Engineering College of Northeast Petroleum University, Daqing 163318, China

Correspondence should be addressed to Wei Ding; dingwei40@126.com

Received 5 September 2018; Revised 12 October 2018; Accepted 28 October 2018; Published 27 January 2019

Academic Editor: Cornelia Vasile

We report herein the synthesis of a novel star-shaped copolymer containing nano-SiO_2 by single-electron transfer living radical polymerization (SET-LRP) in aqueous solution. The effects of polymerization conditions, such as the total amounts and molar ratios of the monomer, initiator, catalyst, ligand, and modified nano-SiO_2, have been investigated through a series of experiments. The prepared acrylamide copolymers have been characterized by FTIR spectroscopy and ^{1}H NMR spectrometry. The properties of the copolymers have been assessed by viscometry and rheometry. The results confirmed that the nano-SiO_2 functional monomer was successfully combined in the SET-LRP. The optimum polymerization conditions were established through orthogonal experiments as a ratio of [AM] : [DMAEMA] : [I] : [CuBr] : [Me_6TREN] of 674.4 : 35.5 : 1 : 1 : 2 at a total concentration of [AM] + [DMAEMA] of 2.5 mol/L. The appropriate concentration of the nano-SiO_2 functional monomer (NSFM) was 0.5 wt% with respect to AM + DMAEMA. The rheology of the star-shaped copolymer exhibited a shear-thickening property when the shear rate exceeded a critical value (100 s^{-1}). The AM/DMAEMA/NSFM copolymer displayed a higher viscosity than AM/DMAEMA at the same concentration. It was found that AM/DMAEMA/NSFM exhibited better salt and temperature tolerances.

1. Introduction

Polymer flooding plays an important role in the field of enhanced oil recovery (EOR) [1, 2]. However, the polyacrylamide (PAM) used has poor temperature and salt tolerances with low shear resistances, making it difficult to adapt to increasingly harsh reservoir conditions.

To address the above problems, researchers have recently sought a technique for modifying oil displacement using polyacrylamide, and to this end, two main strategies have been pursued. The first approach involves the preparation of copolymerizing monomers that can inhibit hydrolysis of the amide group or the introduction of a small amount of hydrophobic functional groups through monomers that can coordinate divalent metal ions, as in the copolymerization of acrylamide (AM) with compounds such as *N*,*N*-dimethylacrylamide, methyl acrylamide, *N*-vinylpyrrolidone (NVP), 2-acrylamido-2-methylpropane sulfonic acid (AMPS), allyl sulfonate, or vinyl sulfonate. The modified polyacrylamide should then display excellent temperature tolerance and salt resistance [3–8]. However, the molecular weights of polymers prepared by various modifications are highly variable, and their performances are fundamentally restricted by their structures, such that it is difficult to obtain satisfactory results. The second approach is to modify the molecular structure through the preparation of dendritic, star-shaped, or hyperbranched polymers, which exhibit excellent shear resistances due to their special reticular structures [9–16]. A special reticular structure can reduce the shear effect on the polymer molecular chain and impart a high-viscosity retention rate. However, the preparation of hyperbranched polymers is relatively complex and incurs high costs.

Cu(0)-mediated living radical polymerization or single-electrontransfer living radical polymerization (Cu(0)-mediated LRP or SET-LRP) is a versatile approach that has long attracted considerable interest. It has been widely used for the synthesis of star-shaped, branched, and hyperbranched polymers in recent years [17–20]. Importantly, it can be efficiently applied to a wide variety of activated monomers (e.g., acrylates, methacrylates, acrylamides, and

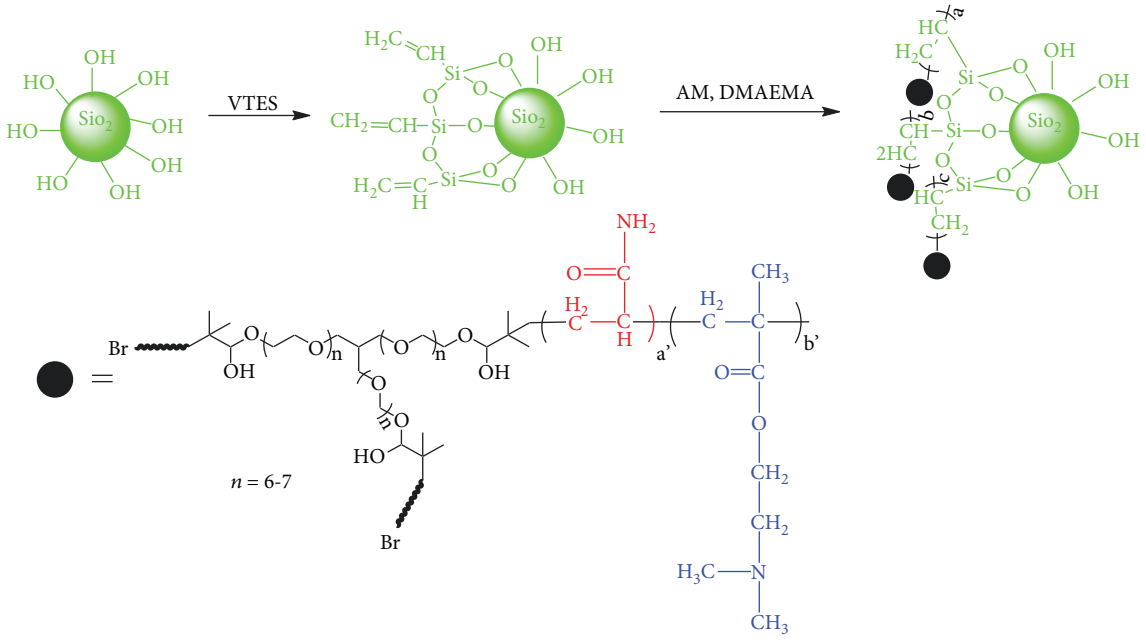

Scheme 1: Synthesis of NSFM and AM/DMAEMA/NSFM.

methacrylamides), as well as nonactivated monomers, such as vinyl chloride, that are not polymerizable by atom-transfer radical polymerization (ATRP).

Recently, many studies have demonstrated that composite materials containing nano-SiO_2 may exhibit favorable properties, such as superior thermal stability, toughness, and strength, owing to the effects of physical adsorption, hydrogen bonding, Si-O bonds, and C-Si bonds [21–25]. In the literature, the synthesis of silica–polymer composites initiated by a SiO_2-Br macroinitiator via SET-LRP has been reported [26–28]. However, to the best of our knowledge, there have been no papers concerning the application of nano-SiO_2 as a monomer in SET-LRP.

In this work, a nano-SiO_2 functional monomer (NSFM) has been introduced into an AM/DMAEMA copolymer by Cu(0)-mediated LRP at room temperature (25°C) with the aim of obtaining more favorable temperature tolerance, salt tolerance, and shear resistance.

2. Experimental

2.1. Chemicals and Reagents. Acrylamide (AM, >99.0% Sinopharm Chemical Reagent, China) was recrystallized twice from acetone prior to use; 2-(dimethylamino)ethyl methacrylate (DMAEMA, 99%) was purchased from Macklin (Shanghai, China) and distilled under reduced pressure before use. Glycerol ethoxylate ($M_n \approx 1000$ g/mol), α-Bromoisobutyryl bromide (BIBB, 98%), triethylamine (TEA, ≥99%), vinyltriethoxysilane (VTES, ≥98.0%), nano-SiO_2 (10-20 nm), and Tris-(2-dimethylaminoethyl) amine (Me_6TERN) were purchased from Sigma-Aldrich and used as received. Water-soluble star initiator (Gly-Br_3) was synthesized as described in the literature [29] and stored at 4°C prior to use. Copper(I) bromide (CuBr, 98%, Sigma-Aldrich) was purified by stirring in acetic acid overnight and washing with copious amounts of ethanol before drying under vacuum to constant weight. All other chemicals and solvents were purchased from Sigma-Aldrich (China) at the highest purity available and used as received unless stated otherwise. Water was deionized by passing through an ion exchange column and doubly distilled.

2.2. Preparation of the Nano-SiO_2 Functional Monomer (NSFM). The nano-SiO_2 functional monomer was synthesized as described in the literature [22]. Firstly, ethanol (83.6 mL), nano-SiO_2 (1.5 g), distilled water (13.6 mL), and aqueous ammonia (1.3 mL) were placed in a 250 mL round-bottomed flask, and the mixture was dispersed by ultrasonication for 30 min. VTES (2.0 mL) was then added to the stirred solution, and reaction was allowed to proceed for 18 h at 30°C. Thereafter, the produced NSFM was separated by centrifugation and washed with distilled water.

The substitution level (ω) of the silica was determined by sodium hydroxide titration. Ground VTS-SiO_2 powder was placed in a 200 mL beaker, and then absolute ethanol (25 mL) and 20 wt% aqueous NaCl solution (75 mL) were added. In order to disperse the VTS-SiO_2, the beaker was ultrasonicated for 10 min. The dispersion system was then adjusted to pH 4 with 0.1 mol/L HCl. Then, 0.1 mol/L aqueous NaOH solution was used to adjust the dispersion system to pH 9. For comparison, dry SiO_2 (2 g) was subjected to the same treatment.

$$\omega = \frac{L_2 - L_1}{L_2} \times 100\%, \quad (1)$$

where L_1 is the volume of NaOH solution consumed by VTS-SiO_2 (mL) and L_2 the volume of NaOH solution consumed by SiO_2 (mL).

In this study, L_1 and L_2 were determined as 9.3 mL and 10.8 mL, respectively; $\omega = 13.9\%$.

2.3. SET-LRP Synthesis of AM/DMAEMA/NSFM. The requisite amount of CuBr was placed in a Schlenk tube equipped with a magnetic stirrer bar and deoxygenated for 20 min. The requisite amount of Me_6TREN was placed in a sealable vial with 1 mL of H_2O and deoxygenated for 15 min (Vial 1). The contents of Vial 1 were then transferred into the Schlenk tube by means of a degassed syringe, and disproportionation was allowed to proceed for 30 min at room temperature (25°C). In another vial (Vial 2), Gly-Br_3, AM, DMAEMA, 0.5 wt% NSFM, and a certain amount of distilled water (total volume 4 mL) were combined and deoxygenated with nitrogen for 15 min. The contents of Vial 2 were then transferred by means of a degassed syringe into the Schlenk tube to start the polymerization. Transfer of the contents of Vial 2 defined t_0. After the desired polymerization time, the solution was immediately filtered to remove copper residues and insoluble impurities. The solution was extensively dialyzed (MWCO = 5000 g/mol) against water for 3 days to remove residual monomer and other small molecules, and then the product was recovered by freeze drying. AM/DMAEMA copolymer was synthesized according to the same method. All copolymers were prepared in partially hydrolyzed form with the same hydrolysis level. The synthetic routes of NSFM and AM/DMAEMA/NSFM were described in Scheme 1.

2.4. Characterization. Infrared (IR) spectra of AM/DMAEMA and AM/DMAEMA/NSFM were measured from samples in KBr pellets on a Perkin-Elmer 1700 spectrometer. The ^{1}H NMR spectrum of AM/DMAEMA/NSFM was recorded on a Bruker DRX spectrometer operated at 500 MHz from a solution of the copolymer in D_2O.

2.5. Rheological Properties and Viscoelasticity. Measurements of the rheology and viscoelasticity of the polymer products were conducted on a Discovery HR-1 rheometer (USA). The shear rate was varied from 2 s^{-1} to 1300 s^{-1}, and the temperature was 30°C, attained at a heating rate of 1.0°C/min. The test system was a binocular tube. A DG41Ti rotor was used for rheological measurements.

3. Results and Discussion

3.1. IR Spectral Analysis. The structures of AM/DMAEMA and AM/DMAEMA/NSFM were fully supported by their IR spectra, as illustrated in Figure 1. The proposed structure of AM/DMAEMA/NSFM, prepared using an acrylamide, dimethylaminoethyl methacrylate, and nano-SiO_2 functional monomer by SET-LRP was confirmed by strong absorptions at $\nu = 3421$ cm^{-1} (–NH stretching vibration), 2929 cm^{-1} (–CH_2 stretching vibration), 1664 cm^{-1} (–C=O stretching vibration), 1452 cm^{-1} (–CH_3 stretching vibration), 1216 cm^{-1} (C–O stretching vibration), 1100 cm^{-1} (Si–O–Si asymmetric stretching vibration) [30, 31], and 640 cm^{-1} (C–Br stretching vibration).

The peak at $\nu = 3421$ cm^{-1} in the IR spectrum of AM/DMAEMA/NSFM was broad, partly due to hydroxyl groups on the nano-SiO_2 surface [31]. As expected, the IR spectrum confirmed the presence of all monomers in AM/DMAEMA/NSFM.

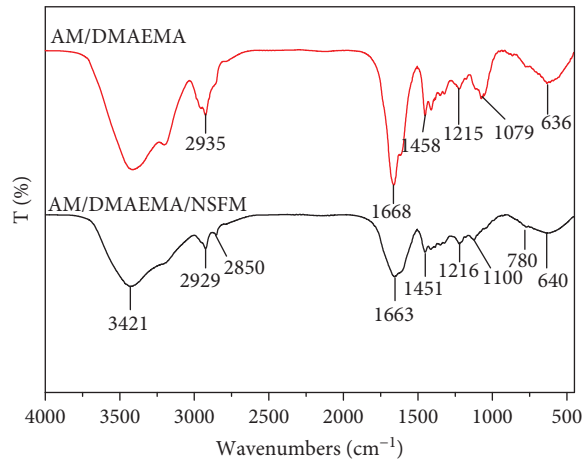

Figure 1: FTIR spectra of AM/DMAEMA and AM/DMAEMA/NSFM copolymers.

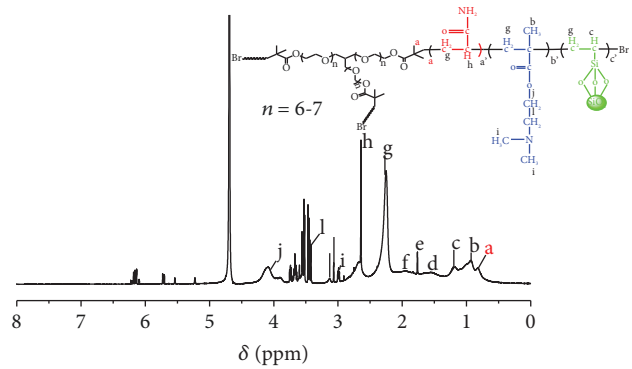

Figure 2: ^{1}H NMR spectrum of AM/DMAEMA/NSFM.

3.2. ^{1}H NMR Analysis. The ^{1}H NMR spectrum of AM/DMAEMA/NSFM is shown in Figure 2. The signals at $\delta = 1.1$–1.3 ppm can be attributed to the protons of type [–CH_2–C**H**(Si(O–)$_3$)–]. The signals at $\delta = 2.1$–2.5 ppm can be assigned to protons of types [–C**H**$_2$–CH($CONH_2$)–], [–C**H**$_2$–CCH_3(COO)–], and [–C**H**$_2$CH(Si(O–)$_3$)–]. The protons of type [–CH_2–C**H**($CONH_2$)–] give rise to signals at $\delta = 2.5$–2.9 ppm. The signals at $\delta = 2.8$–3.0 ppm can be ascribed to the [–N(CH_3)$_2$] protons. Signals in the region $\delta = 6.0$–6.3 ppm can be ascribed to [–OH] on the NSFM. No signal due to -NH_2 is seen in the ^{1}H NMR spectrum, because these protons are labile and exchange with the solvent.

The spectrometric analysis confirmed that each of the monomers successfully participated in the SET-LRP.

3.3. SET-LRP of AM, DMAEMA, and NSFM in H_2O

3.3.1. Conditions for Terpolymerization. Orthogonal experiments (L5^4) were arranged to investigate the main effects

Table 1: Factors of the orthogonal experiments ($L5^4$).

Levels	1	2	3	4
Total monomer concentration ($mol \cdot L^{-1}$)	1.5	2.5	3.5	4.5
Amount of initiator (g)	0.0075	0.0150	0.0225	0.0300
Amount of catalyst (g)	0.0011	0.0018	0.0025	0.0033
Amount of ligand (μL)	4	7	10	13
The molar ratio of monomers	95 : 5	85 : 15	75 : 25	60 : 40

Table 2: Results of the orthogonal experiments ($L5^4$).

No.	Total monomer concentration ($mol \cdot L^{-1}$)	The molar ratio of monomers	Amount of initiator (g)	Amount of catalyst (g)	Amount of ligand (μL)	Viscosity (mPa·s)
1	1.5	95 : 5	0.0075	0.0011	4	6.7
2	1.5	85 : 15	0.0150	0.0018	7	5.6.
3	1.5	75 : 25	0.0225	0.0025	10	6.3
4	1.5	60 : 40	0.0300	0.0033	13	7.8
5	2.5	95 : 5	0.0150	0.0025	13	17.4
6	2.5	85 : 15	0.0075	0.0033	10	10.1
7	2.5	75 : 25	0.0300	0.0011	7	7.8
8	2.5	60 : 40	0.0225	0.0018	4	9.2
9	3.5	95 : 5	0.0225	0.0033	7	3.1
10	3.5	85 : 15	0.0300	0.0025	4	5.5
11	3.5	75 : 25	0.0075	0.0018	13	7.8
12	3.5	60 : 40	0.0150	0.0011	10	5.8
13	4.5	95 : 5	0.0300	0.0018	10	14.6
14	4.5	85 : 15	0.0225	0.0011	13	14.9
15	4.5	75 : 25	0.0150	0.0033	4	5.8
16	4.5	60 : 40	0.0075	0.0025	7	9.2
K1	6.6	10.4	8.4	8.8	6.8	
K2	11.2	9.1	8.7	9.3	6.4	
K3	5.6	7.0	8.4	9.6	9.2	
K4	11.2	8.0	9.0	6.7	11.9	
R	5.6	3.4	0.6	2.9	5.5	

Note: the addition of NSFM is 0.5% of the total mass of monomers; K1: average viscosity of level one; K2: average viscosity of level two; K3: average viscosity of level three; K4: average viscosity of level four; *R*: range.

(see Table 1) of the total monomer concentration; the amounts of initiator, catalyst, and ligand; and the molar ratio of monomers, on the viscosity of the resulting copolymer. Polymer solutions at a concentration of 2 g/L were prepared in deionized water. The viscosities of these solutions were measured by means of a Brookfield DV-II viscometer (USA) at $T = 30^{\circ}C$ using a no. 63 rotor (rotation speed: 30 rpm). Higher viscosity indicated better performance. From the results of orthogonal experiments shown in Table 2, the optimal polymerization conditions were obtained as follows: total monomer concentration 2.5 mol/L, molar ratio of monomers (AM/DMAEMA), 95 : 5; amount of initiator, 0.0300 g; amount of catalyst, 0.0025 g; amount of ligand 13 μL, namely, [AM] + [DMAEMA] = 2.5 mol/L; [AM] : [DMAEMA] : [I] : [CuBr] : [Me_6TREN] = 674.4 : 35.5 : 1 : 1 : 2.

The optimally synthesized sample had a viscosity of 19.50 mPa·s under the same test conditions. Comparing the *R* values associated with five factors, it was found that their impacts increased in the following sequence: amount of initiator < amount of catalyst < molar ratio of monomers < amount of ligand < total monomer concentration. We also investigated the effect of the amount of NSFM on the viscosity of the copolymer.

3.3.2. Effect of NSFM Dosage. Based on Figures 1 and 2, it is clear that NSFM successfully participated in the SET-LRP. The effect of the dosage of NSFM on the viscosity of the product was investigated, and the results are presented in Figure 3.

It can be seen from Figure 3 that the viscosity of the copolymer first increased and then decreased with increasing NSFM content. The maximum viscosity of 19.5 mPa·s was seen with an NSFM loading of 0.5 wt%. This may have been due to the terpolymer having the maximum molecular weight at this point.

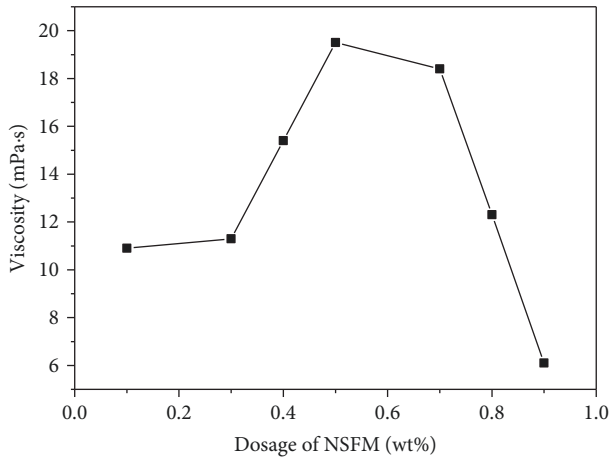

Figure 3: Effect of the dosage of NSFM on the performance of AM/DMAEMA/NSFM; [AM] + [DMAEMA] = 2.5 mol/L, [AM] : [DMAEMA] : [I] : [CuBr] : [Me_6TREN] = 674.4 : 35.5 : 1 : 1 : 2.

When the dosage of NSFM was less than 0.5 wt%, more monomers polymerized to form hyperbranched products. With the addition of NSFM, the hydrodynamic volume of the molecules increased, the molecules became interwoven to form more high-strength reticular structures, and as a result, the solution viscosity increased. With the addition of more than 0.5 wt% NSFM, more branched products and shorter molecular chains were formed. As a result, the molecular weight of the polymer decreased, the entanglement between molecules became weak, the hydrodynamic volumes of the molecules decreased, and the solution viscosity decreased.

3.4. Temperature Tolerance. For the samples used to assess temperature tolerance, salt resistance, and shear resistance, the composition of the reagents for producing the AM/DMAEMA copolymer was 95 mol% AM and 5 mol% DMAEMA. The composition of the reagents for the preparation of the AM/DMAEMA/NSFM copolymer was 89 wt% AM, 10.5 wt% DMAEMA, and 0.5 wt% NSFM (the molar ratio of AM to DMAEMA was still 95 : 5).

AM/DMAEMA and AM/DMAEMA/NSFM solutions were prepared in distilled water. The viscosities of the copolymer solutions were measured by means of a Brookfield DV-II+ viscometer at different temperatures. The viscosity versus temperature curves of the AM/DMAEMA and AM/DMAEMA/NSFM solutions are shown in Figure 4. The results show that the introduction of NSFM improved the thermostability of the copolymer. With increasing temperature, the viscosities of the two kinds of polymers gradually decreased to different levels. The AM/DMAEMA/NSFM solution consistently showed higher viscosity compared to that of the AM/DMAEMA solution. However, the viscosity of the AM/DMAEMA/NSFM solution decreased less than that of the AM/DMAEMA solution when the temperature exceeded 50°C. It was also found that AM/DMAEMA/NSFM could achieve up to 47.1% viscosity retention at 90°C, whereas AM/DMAEMA showed just 14.2% viscosity retention at this temperature. This lends support to the view

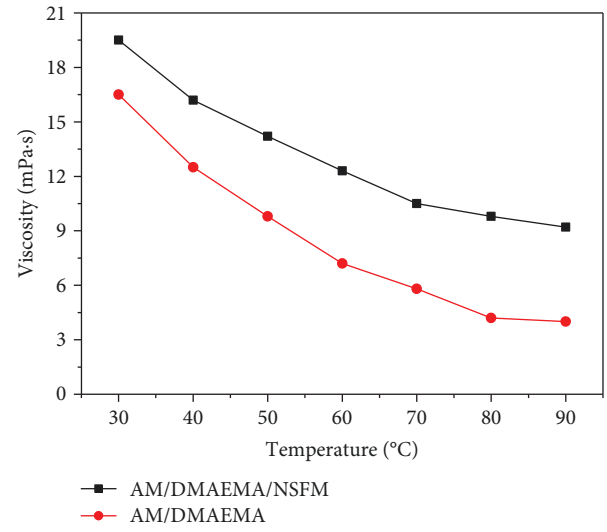

Figure 4: Viscosity versus temperature for AM/DMAEMA and AM/DMAEMA/NSFM solutions. The viscosities of copolymer solutions (0.2 wt%) were measured with a Brookfield DV-II viscometer using a no. 63 rotor (rotation speed: 30 rpm).

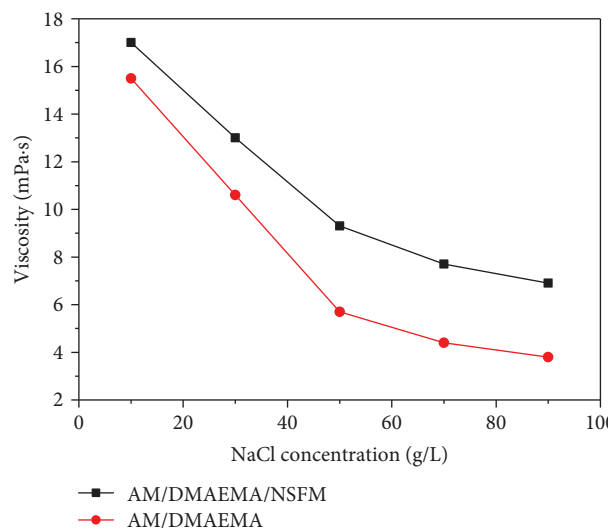

Figure 5: Salt tolerances of AM/DMAEMA and AM/DMAEMA/NSFM solutions (0.2 wt%) at 30°C. The viscosities of copolymer solutions (0.2 wt%) were measured with a Brookfield DV-II viscometer using a no. 63 rotor (rotation speed: 30 rpm).

that stable Si-O and C-Si bonds improve the temperature tolerance of AM/DMAEMA/NSFM.

3.5. Salt Tolerance. The influences of electrolyte concentration on the viscosities of AM/DMAEMA and AM/DMAEMA/NSFM solutions are shown in Figure 5. With increasing NaCl concentration, the viscosities of the copolymer solutions gradually decreased. This could be attributed to compression of the diffuse electric double layer of the carboxylate ions by electrolyte ions, thereby decreasing the

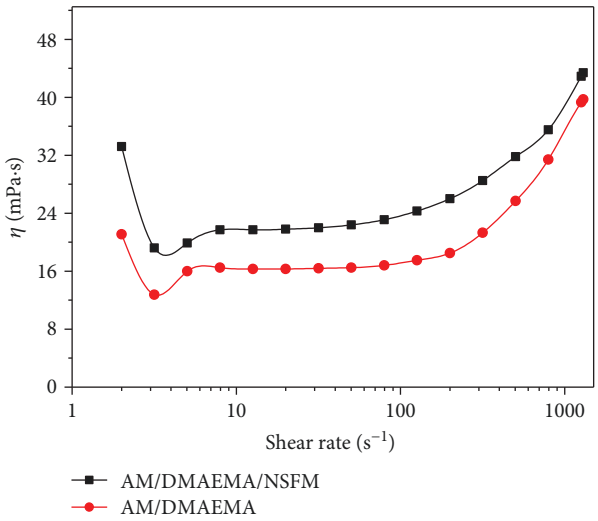

Figure 6: Effect of shear rate on the viscosities of AM/DMAEMA and AM/DMAEMA/NSFM solutions. The copolymer solutions (0.2 wt%) were prepared in distilled water.

electrostatic repulsive force [17]. The polymer chains are in a coiled rather than extended conformation, which leads to a decrease in viscosity. Compared with AM/DMAEMA, AM/DMAEMA/NSFM exhibited better salt tolerance. This could be attributed to the hyperbranched structure of the modified nanostar polymer molecule. The reticular structure formed in the solution can weaken the shielding effect of the small-molecule electrolyte on the charge of the copolymer molecular chain to some extent, reducing the crimp degree of the molecular chains, thereby improving the salt-resisting property of the copolymer.

3.6. Shear Resistance. Viscosity versus shear rate curves for AM/DMAEMA and AM/DMAEMA/NSFM are shown in Figure 6. At lower shear rates, the viscosities of the copolymer solutions decreased slightly. On increasing the shear rate from 2 to 100 s^{-1}, the viscosities of the copolymer solutions remained essentially constant but then increased when the shear rate exceeded 100 s^{-1}.

This may have been due to the hyperbranched structures of the copolymers. The results also indicated that AM/DMAEMA/NSFM had better viscosifying property than AM/DMAEMA, and the viscosity of the former was higher than that of the latter at shear rates less than 100 s^{-1}.

At a certain shear rate, shear stress destroys the intramolecular associative structure of polymer molecules, and the viscosity of a solution decreases. Conversely, due to expansion and extension of the polymer chains, intermolecular association increases the viscosity of the solution. As the net result of these two effects, the solutions showed either a slight decrease or no change in viscosity. At a high shear rate, however, the molecular chains of the polymers were highly stretched in a short time, resulting in intermolecular association. Hence, the viscosity of the polymer solution was increased, and shear thickening occurred.

4. Conclusions

A novel terpolymer containing nano-SiO_2 has been synthesized at ambient temperature by SET-LRP, employing a nano-SiO_2 functional monomer. The product has been characterized by FTIR spectroscopy and ^{1}H NMR spectrometry. The optimum polymerization conditions were identified as an [AM] : [DMAEMA] : [I] : [CuBr] : [Me_6TREN] ratio of 674.4 : 35.5 : 1 : 1 : 2 in a total concentration of [AM] + [DMAEMA] of 2.5 mol/L, with a concentration of NSFM of 0.5 wt% (with respect to AM + DMAEMA). The rheology of the copolymer displayed shear thickening above a critical shear rate (100 s^{-1}). The AM/DMAEMA/NSFM copolymer showed a higher viscosity retention of 47.1% than AM/DMAEMA (14.2%) at the same concentration. The copolymer containing nano-SiO_2 also exhibited better salt tolerance. AM/DMAEMA/NSFM would thus be expected to enhance oil recovery in high-temperature, high-salinity, and low-permeability reservoirs.

Data Availability

The infrared (IR) spectra and ^{1}H NMR data used to support the nano-SiO2 functional monomer which successfully participated in SET-LRP are included within the article. Data used to support the optimum reaction conditions of polymerization findings of this study are included within the article. The rheology data of the star-shaped copolymer were also listed in the article.

Conflicts of Interest

The authors declare that they have no competing interests.

Acknowledgments

We are grateful for the financial support from the National Nature Science Foundation of China (51474068) which funded the present study. We thank International Science Editing (http://www.internationalscienceediting.com) for editing this manuscript.

References

[1] S. Mahran, A. Attia, and B. Saha, *Proceedings of 11th International Sustainable Energy & Environmental Protection Conference: A Review on Polymer Flooding in Enhanced Oil Recovery under Harsh Conditions*, Paisley, Scotland, 2018.

[2] J. J. Sheng, B. Leonhardt, and N. Azri, "Status of polymer-flooding technology," *Journal of Canadian Petroleum Technology*, vol. 54, no. 2, pp. 116–126, 2015.

[3] Z. Ye, G. Gou, S. Gou, W. Jiang, and T. Liu, "Synthesis and characterization of a water-soluble sulfonates copolymer of acrylamide and N-allylbenzamide as enhanced oil recovery chemical," *Journal of Applied Polymer Science*, vol. 128, no. 3, pp. 2003–2011, 2012.

[4] A. Sabhapondit, A. Borthakur, and I. Haque, "Water soluble acrylamidomethyl propane sulfonate (AMPS) copolymer as an enhanced oil recovery chemical," *Energy and Fuels*, vol. 17, no. 3, pp. 683–688, 2003.

[5] C.-S. Yang, K. Shin, and H. K. Jeong, "Thermal analysis of poly(sodium 4-styrenesulfonate) intercalated graphite oxide composites," *Chemical Physics Letters*, vol. 517, no. 4–6, pp. 196–198, 2011.

[6] X.-J. Liu, W.-C. Jiang, S.-H. Gou, Z. B. Ye, and X. D. Xie, "Synthesis and evaluation of a water-soluble acrylamide binary sulfonates copolymer on MMT crystalline interspace and EOR," *Journal of Applied Polymer Science*, vol. 125, no. 2, pp. 1252–1260, 2012.

[7] X. Liu, W. Jiang, S. Gou, Z. Ye, and C. Luo, "Synthesis and clay stabilization of a water-soluble copolymer based on acrylamide, modular β-cyclodextrin, and AMPS," *Journal of Applied Polymer Science*, vol. 128, no. 5, pp. 3398–3404, 2013.

[8] X. Liu, W. Jiang, S. Gou et al., "Synthesis and evaluation of novel water-soluble copolymers based on acrylamide and modular β-cyclodextrin," *Carbohydrate Polymers*, vol. 96, no. 1, pp. 47–56, 2013.

[9] D. A. Tomalia, H. Baker, J. Dewald et al., "A new class of polymers: starburst-dendritic macromolecules," *Polymer Journal*, vol. 17, no. 1, pp. 117–132, 1985.

[10] D. A. Tomalia, H. Baker, J. Dewald et al., "Dendritic macromolecules: synthesis of starburst dendrimers," *Macromolecules*, vol. 19, no. 9, pp. 2466–2468, 1986.

[11] J. C. Hummelen, J. L. J. Van Dongen, and E. W. Meijer, "Electrospray mass spectrometry of poly(propylene imine) dendrimers—the issue of dendritic purity or polydispersity," *Chemistry*, vol. 3, no. 9, pp. 1489–1493, 1997.

[12] L. J. Twyman, A. E. Beezer, R. Esfand, M. J. Hardy, and J. C. Mitchell, "The synthesis of water soluble dendrimers, and their application as possible drug delivery systems," *Tetrahedron Letters*, vol. 40, no. 9, pp. 1743–1746, 1999.

[13] M. S. Diallo, S. Christie, P. Swaminathan et al., "Dendritic chelating agents. 1. Cu(II) binding to ethylene diamine core poly(amidoamine) dendrimers in aqueous solutions," *Langmuir*, vol. 20, no. 7, pp. 2640–2651, 2004.

[14] L. Xue, U. S. Agarwal, M. Zhang et al., "Synthesis and direct topology visualization of high-molecular-weight star PMMA," *Macromolecules*, vol. 38, no. 6, pp. 2093–2100, 2005.

[15] D. S. Achilleos, T. K. Georgiou, and C. S. Patrickios, "Amphiphilic model conetworks based on cross-linked star copolymers of benzyl methacrylate and 2-(dimethylamino)ethyl methacrylate: synthesis, characterization, and DNA adsorption studies," *Biomacromolecules*, vol. 7, no. 12, pp. 3396–3405, 2006.

[16] X. Wang, Y. Zhang, T. Li, W. Tian, Q. Zhang, and Y. Cheng, "Generation 9 polyamidoamine dendrimer encapsulated platinum nanoparticle mimics catalase size, shape, and catalytic activity," *Langmuir*, vol. 29, no. 17, pp. 5262–5270, 2013.

[17] M. R. Whittaker, C. N. Urbani, and M. J. Monteiro, "Synthesis of linear and 4-arm star block copolymers of poly(methyl acrylate-b-solketal acrylate) by SET-LRP at 25 °C," *Journal of Polymer Science Part A: Polymer Chemistry*, vol. 46, no. 18, pp. 6346–6357, 2008.

[18] W. Zhang, W. Zhang, J. Zhu, Z. Zhang, and X. Zhu, "Controlled synthesis of pH-responsive amphiphilic A2B2miktoarm star block copolymer by combination of SET-LRP and RAFT polymerization," *Journal of Polymer Science Part A: Polymer Chemistry*, vol. 47, no. 24, pp. 6908–6918, 2009.

[19] W. Ding, C. Lv, Y. Sun, H. Luan, T. Yu, and G. Qu, "Synthesis of star polymethyl acrylate by SET-LRP at ambient temperature," *Polymer Bulletin*, vol. 67, no. 8, pp. 1499–1505, 2011.

[20] Q. Zhang, P. Wilson, Z. Li et al., "Aqueous copper mediated living polymerization: exploiting rapid disproportionation of CuBr with Me_6TREN," *Journal of the American Chemical Society*, vol. 135, no. 19, pp. 7355–7363, 2013.

[21] Z. Ye, X. Qin, N. Lai, Q. Peng, X. Li, and C. Li, "Synthesis and performance of an acrylamide copolymer containing nano-SiO2 as enhanced oil recovery chemical," *Journal of Chemistry*, vol. 2013, Article ID 437309, 10 pages, 2013.

[22] X. Wang, X. Zhao, M. Wang, and Z. Shen, "The effects of atomic oxygen on polyimide resin matrix composite containing nanosilicon dioxide," *Nuclear Instruments and Methods in Physics Research B*, vol. 243, no. 2, pp. 320–324, 2006.

[23] V. A. Bershtein, L. M. Egorova, P. N. Yakushev, P. Pissis, P. Sysel, and L. Brozova, "Molecular dynamics in nanostructured polyimide–silica hybrid materials and their thermal stability," *Journal of Polymer Science Part B: Polymer Physics*, vol. 40, no. 10, pp. 1056–1069, 2002.

[24] N. D. Alberola, K. Benzarti, C. Bas, and Y. Bomal, "Interface effects in elastomers reinforced by modified precipitated silica," *Polymer Composites*, vol. 22, no. 2, pp. 312–325, 2001.

[25] A. Voronov, A. Kohut, A. Synytska, and W. Peukert, "Mechanochemical modification of silica with poly(1-vinyl-2-pyrrolidone) by grinding in a stirred media mill," *Journal of Applied Polymer Science*, vol. 104, no. 6, pp. 3708–3714, 2007.

[26] X. Liu, D. Appelhans, T. Zhang, and B. Voit, "Rapid synthesis of dual-responsive hollow capsules with controllable membrane thickness by surface-initiated SET-LRP polymerization," *Macromolecules*, vol. 51, no. 3, pp. 1011–1019, 2018.

[27] T. K. L. Nguyen, X. T. Cao, Y. T. Jeong, H. Heo, Y. S. Gal, and K. T. Lim, "Synthesis and characterization of core-shell type silica-polymer composites by surface-initiated SET-LRP," *Molecular Crystals and Liquid Crystals*, vol. 654, no. 1, pp. 174–180, 2017.

[28] C. Heng, M. Liu, K. Wang et al., "Fabrication of silica nanoparticle based polymer nanocomposites via a combination of mussel inspired chemistry and SET-LRP," *RSC Advances*, vol. 5, no. 111, pp. 91308–91314, 2015.

[29] R. Aksakal, M. Resmini, and C. R. Becer, "Pentablock star shaped polymers in less than 90 minutes via aqueous SET-LRP," *Polymer Chemistry*, vol. 7, no. 1, pp. 171–175, 2016.

[30] G.-H. Hsiue, W.-J. Kuo, Y.-P. Huang, and R.-J. Jeng, "Microstructural and morphological characteristics of PS–SiO2 nanocomposites," *Polymer*, vol. 41, no. 8, pp. 2813–2825, 2000.

[31] B. J. Kim and K. S. Kang, "Fabrication of a crack-free large area photonic crystal with colloidal silica spheres modified with vinyltriethoxysilane," *Crystal Growth & Design*, vol. 12, no. 8, pp. 4039–4042, 2012.